Efimov Physics Around the Neutron-Rich ^{60}Ca Isotope

G. Hagen,[1,2] P. Hagen,[3] H.-W. Hammer,[3] and L. Platter[4,5]

[1]*Physics Division, Oak Ridge National Laboratory, Oak Ridge, Tennessee 37831, USA*
[2]*Department of Physics and Astronomy, University of Tennessee, Knoxville, Tennessee 37996, USA*
[3]*Helmholtz-Institut für Strahlen- und Kernphysik (Theorie) and Bethe Center for Theoretical Physics, Universität Bonn, 53115 Bonn, Germany*
[4]*Argonne National Laboratory, Physics Division, Argonne, Illinois 60439, USA*
[5]*Department of Fundamental Physics, Chalmers University of Technology, SE-412 96 Gothenburg, Sweden*

(Received 18 June 2013; published 23 September 2013)

We calculate the neutron-^{60}Ca S-wave scattering phase shifts using state of the art coupled-cluster theory combined with modern *ab initio* interactions derived from chiral effective theory. Effects of three-nucleon forces are included schematically as density dependent nucleon-nucleon interactions. This information is combined with halo effective field theory in order to investigate the ^{60}Ca-neutron-neutron system. We predict correlations between different three-body observables and the two-neutron separation energy of ^{62}Ca. This provides evidence of Efimov physics along the calcium isotope chain. Experimental key observables that facilitate a test of our findings are discussed.

DOI: 10.1103/PhysRevLett.111.132501 PACS numbers: 21.10.Gv, 21.60.−n, 27.50.+e

Introduction.—The emergence of new degrees of freedom is one of the most important aspects of the physics along the neutron (n) drip line. For example, halo nuclei are characterized by a tightly bound core (c) and weakly bound valence nucleons [1–4] and thus display a reduction in the effective degrees of freedom. They are usually identified by an extremely large matter radius or a sudden decrease in the one- or two-nucleon separation energy along an isotope chain. The features of these halos are universal if the small separation energy of the valence nucleons is associated with a large S-wave scattering length. These phenomena are then independent of the details of the microscopic interaction and occur in a large class of systems in atomic, nuclear, and particle physics [5,6]. For a three-body system (e.g., core-nucleon-nucleon) interacting through a large S-wave scattering length, Efimov showed that the system will display discrete scale invariance [7]. This discrete scale invariance is exact in the limit of zero-range interactions and infinite scattering lengths. For fixed finite values of the scattering length and range, it is approximate. The hallmark feature of this so-called Efimov effect is a tower of bound states. The ratio of the binding energies of successive states is characterized by a discrete scaling factor. This scaling factor is approximately 515 in the case of identical bosons. Systems whose particles have different masses will generally have a smaller scaling factor. It can be obtained by the solving of a transcendental equation [5].

Several nuclear systems have been discussed as possible candidates for Efimov states. The most promising system known so far is the ^{22}C halo nucleus which was found to display an extremely large matter radius [8] and is known to have a significant S-wave component in the n-^{20}C system [9]. See Ref. [10] for a recent study of Efimov physics in ^{22}C.

Whether heavier two-neutron halos exist is still an open question. Recently, there has been much interest, both experimentally and theoretically, in determining precise values for masses, understanding shell evolution and the location of the dripline in the neutron rich calcium isotopes [11–14]. Coupled-cluster calculations of neutron rich calcium isotopes that included coupling to the scattering continuum and schematic three-nucleon forces, suggested that there is an inversion of the gds shell-model orbitals in ^{53,55,61}Ca. In particular it was suggested that a large S-wave scattering length might occur in ^{61}Ca with interesting implications for ^{62}Ca.

A conclusive statement on whether a halo is an Efimov state can generally only be made if a sufficient number of observables is known and if those fulfill relations dictated by universality. However, typically only a very limited number of observables in these systems is accessible experimentally. Recently, significant progress has been made in microscopic calculations of low-energy nucleon-nucleus scattering properties starting from realistic nucleon-nucleon interactions [15–18]. In this Letter, we use the coupled-cluster method [19] combined with modern chiral effective theory interactions and follow the method outlined in Ref. [15] to compute the elastic scattering of neutrons on ^{60}Ca. We analyze the resulting phase shift data to obtain quantitative estimates for the scattering length and the effective range and show that a large scattering length can be expected in this system. The results obtained from *ab initio* calculations are then used as input for the so-called halo effective field theory (EFT) that describes the halo system in terms of its effective degrees of freedom (core and valence nucleons) [20,21]. We use halo EFT to analyze the implications of the coupled cluster results for the ^{60}Ca-n-n system. Specifically, we focus on

the signals of Efimov physics that are a consequence of the large scattering length in the ^{60}Ca-n and n-n systems.

Hamiltonian and method.—We perform coupled-cluster calculations for ^{60,61}Ca starting from the intrinsic A-nucleon Hamiltonian,

$$\hat{H} = \sum_{1\le i<j\le A}\left(\frac{(\mathbf{p}_i - \mathbf{p}_j)^2}{2mA} + \hat{V}_{NN}^{(i,j)} + \hat{V}_{\mathrm{3Neff}}^{(i,j)}\right). \quad (1)$$

Here, the intrinsic kinetic energy depends on the mass number A. The potential $\hat{V}_{NN}$ denotes the chiral NN interaction at next-to-next-to-next-to leading order [22,23] (with cutoff $\Lambda = 500$ MeV), and $\hat{V}_{\mathrm{3Neff}}$ is a schematic potential based on the in-medium chiral NN interaction by Holt *et al.* [24]. The potential $\hat{V}_{\mathrm{3Neff}}$ results from integrating one nucleon in the leading-order chiral three-nucleon force (3NF) over the Fermi sphere with Fermi momentum k_F in symmetric nuclear matter. In this work we employ the 3NF parameters which were used to study shell evolution in neutron rich calcium isotopes [13], and for proton elastic scattering on ^{40}Ca [15]. This interaction predicts well the masses for ^{50,51}Ca [11] and low-lying states in ^{53,54}Ca [25], but is probably lacking in total binding energy for isotopes around ^{60}Ca. To describe elastic scattering of a nucleon on a nucleus A, we compute the one-nucleon overlap function between the ground state of the nucleus A with the scattering solutions of the $A+1$ nucleus $O_A^{A+1}(lj;kr) = \sum_n \langle A+1\|\tilde{a}^\dagger_{nlj}\|A\rangle \phi_{nlj}(r)$, with the integral sum over bound and scattering states (see Ref. [15] for more details). To obtain the ground state of nucleus A, we use the coupled-cluster method in the singles-and-doubles approximation (CCSD). For the excited states of $A+1$, we use particle-attached equation-of-motion coupled-cluster theory truncated at the two-particle-one-hole excitation level [26]. We solve the coupled-cluster equations using a Hartree-Fock basis built from $N_{\max} = 17$ major spherical oscillator shells and 50 Woods-Saxon discretized scattering states for the S wave [15]. We use the harmonic oscillator frequencies $\hbar\omega = 20$, 24, 28 MeV to gauge the convergence of our calculations.

We compute the radial overlap function $O_A^{A+1}(lj;kr)$ following the method outlined in Ref. [27] and the elastic scattering phase shifts following the procedure described in [15]. This amounts to matching the computed scattering one-nucleon overlap functions to known asymptotic forms given by spherical Bessel and Neumann functions. In Fig. 1, we show the computed S-wave elastic scattering phase shifts for an incoming neutron on the 0^+ ground state of ^{60}Ca for different harmonic oscillator frequencies. The corresponding CCSD ground state energy for ^{60}Ca shows a weak dependence on the harmonic oscillator frequency, and we get -386.07 MeV, -390.66 MeV, and -388.62 MeV for $\hbar\omega = 20$, 24, 28 MeV, respectively. For $\hbar\omega = 20$ and 24 MeV, ^{61}Ca supports a very weakly bound state, and the computed separation energy is 8 and 5 keV, respectively. For $\hbar\omega = 28$ MeV, ^{61}Ca is just barely unbound. In order to quantify the sensitivity of our results on the parameters of our effective interaction, we varied the Fermi momentum k_F in our schematic 3NF by ± 0.01 fm^{-1} away from the optimal value $k_F = 0.95$ fm^{-1} [13]. We found that the total binding energy of ^{60}Ca varied with ± 1 MeV and the separation energy of ^{61}Ca varied with ± 3 keV. The uncertainty in our results coming from the tuned parameters of our schematic 3NF is therefore of the same order as the uncertainty coming from the finite size of the single-particle basis used. Regarding the accuracy of our computed separation energy of ^{61}Ca we found that the $J^\pi = 1/2^+$ state is dominated (more than 95%) by one-particle excitations. This gives us confidence that the ^{61}Ca separation energy is much more accurately computed than the total binding energy (which might be more sensitive to correlations beyond the CCSD approximation). In Ref. [13] one of us computed the $J^\pi = 5/2^+$, $9/2^+$ excited states in ^{61}Ca, and found them to be resonances with energies $E_{5/2^+} = 1.14 - 0.31i$ MeV and $E_{9/2^+} = 2.19 - 0.01i$ MeV with respect to the neutron emission threshold. Our results for S-wave elastic scattering of neutrons on ^{60}Ca therefore strongly support the ground state of ^{61}Ca having $J^\pi = 1/2^+$.

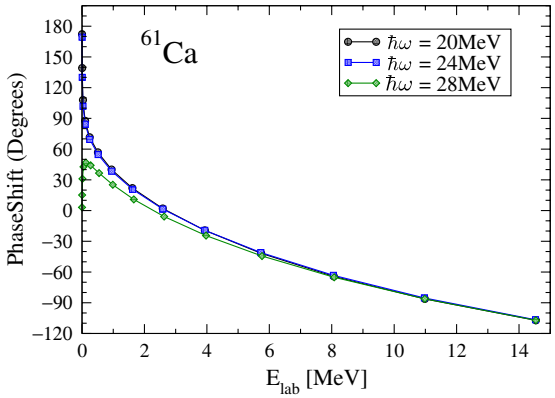

FIG. 1 (color online). S-wave phase shifts for n-^{60}Ca scattering from the coupled-cluster method as a function of the neutron energy in the lab frame for $\hbar\omega = 20$, 24, 28 MeV.

Scattering parameters.—The scattering phase shift data obtained as described above, provides the input parameters required for a halo EFT analysis. For low energies, the phase shifts for neutron-core scattering can be represented by the effective range expansion $k\cot\delta_{cn} = -(1/a_{cn}) + (r_{cn}/2)k^2 + \cdots$, where k is the momentum in the center-of-mass frame and the ellipses denote higher order terms in the expansion. We have fitted the phase shift data by polynomials in k^2 and extracted the scattering length a_{cn} and effective range r_{cn}. The errors from the degree of the fitted polynomials are negligible to the given accuracy. We obtained the scattering parameters displayed in Table I.

TABLE I. Extracted ^{60}Ca-n scattering length a_{cn} (1st column) and effective range r_{cn} (2nd column) for different oscillator parameters $\hbar\omega$. The neutron separation energy S_n and the estimated breakdown scale $S_{\rm deep}$ are given in the 3rd and 4th column, respectively.

$\hbar\omega$ (MeV)	a_{cn} (fm)	r_{cn} (fm)	S_n (keV)	$S_{\rm deep}$ (keV)
20	55.0	8.8	8.4	544
24	53.2	9.1	5.3	509
28	−26.1	10.8	⋯	361

For $\hbar\omega = 28$ MeV, the scattering length is negative and the ^{61}Ca system is unbound. This could indicate that the implicit infrared cutoff in the harmonic oscillator basis for $\hbar\omega = 28$ MeV is too large to resolve threshold scattering. While halo EFT could in principle be applied, there are fewer observables in this case. Thus, we do not use these data in our analysis below. For $\hbar\omega = 20$ and 24 MeV, we find consistent results. The scattering length is enhanced by about a factor of six compared to the effective range. In the following, we will use the average of the results for $\hbar\omega = 20$ and 24 MeV and take their spread as an optimistic error estimate, i.e.,

$$a_{cn} = 54(1)\ \text{fm} \quad \text{and} \quad r_{cn} = 9.0(2)\ \text{fm}. \tag{2}$$

The inverse effective range can be taken as an estimate of the breakdown momentum beyond which the halo EFT cannot be applied anymore. The corresponding energy scale $S_{\rm deep} = 1/(\mu_{cn} r_{cn}^2)$, where μ_{cn} is the reduced mass of the cn system is given in the 4th column of Table I.

Halo EFT.—Halo EFT provides a model-independent description of halo nuclei using the effective degrees of freedom of these systems, i.e., the core and the valence nucleons. Based on the previous analysis, we will assume that the interaction is short ranged with $R \sim r_{cn}$. The expansion parameter of the EFT is R divided by the large scattering length a_{cn}. The ^{60}Ca-n interaction is described by a spin-1/2 dimer field $(\vec{d}_{cn})^T = (d_{cn,\uparrow}, d_{cn,\downarrow})$. The interaction of the two neutrons is described by a spin-0 dimer field d_{nn}. They have to be in the spin-singlet channel since they only interact in the S wave. To leading order in R/a, the Lagrangian is then [28]

$$\begin{aligned}\mathcal{L} = {} & \psi_c^\dagger\left(i\partial_0 + \frac{\nabla^2}{2M}\right)\psi_c + \vec{\psi}_n^\dagger\left(i\partial_0 + \frac{\nabla^2}{2m}\right)\vec{\psi}_n \\ & + \Delta_{nn} d_{nn}^\dagger d_{nn} + \Delta_{cn}\vec{d}_{cn}^\dagger\vec{d}_{cn} + h d_{nn}^\dagger \psi_c^\dagger \psi_c d_{nn} \\ & - \left[g_{cn}\vec{d}_{cn}^\dagger\vec{\psi}_n\psi_c + \frac{g_{nn}}{2} d_{nn}^\dagger(\vec{\psi}_n^{\rm T} P \vec{\psi}_n) + \text{H.c}\right] + \cdots,\end{aligned} \tag{3}$$

where the ψ_c and ψ_n denote the core and neutron fields, respectively, the ellipses denote higher-order terms and P projects on the spin singlet and the ellipses denote higher-order terms. The coupling constants g_i and Δ_i are fitted to the effective range parameters of the n-n and ^{60}Ca-n system. Once this is done, various two-body observables can be calculated. For example, the charge radius of a general one-neutron halo with pointlike core to next-to-leading order is [29]

$$\langle r_E^2\rangle_{\rm rel} = \frac{f^2}{2\gamma_{cn}^2(1 - r_{cn}\gamma_{cn})}, \tag{4}$$

where $f = \mu_{cn}/M$, M is the core mass, and γ_{cn} the binding momentum of the cn system. The total charge radius of ^{61}Ca is then obtained by adding this value to the charge radius of ^{60}Ca $\langle r_E^2\rangle_{^{61}\text{Ca}} = \langle r_E^2\rangle_{^{60}\text{Ca}} + \langle r_E^2\rangle_{\rm rel}$. Using the scattering length and effective range from Eq. (2), we obtain, $\langle r_E^2\rangle_{\rm rel} = 0.39(2)$ fm^2 where the error is from the uncertainty in a_{cn} and higher order corrections are estimated to be of order $(r_{cn}/a_{cn})^2 \sim 3\%$. We note that the possible existence of a low-lying excited state in ^{60}Ca might introduce new parameters in halo EFT and thereby alter the relations among ^{62}Ca properties discussed below.

Extending the framework of Ref. [29] to an external current that couples to the matter distribution, we have calculated the matter radius of a one-neutron halo. Normalizing the matter form factor to unity, we find for the relative matter radius to next-to leading order

$$\langle r_{\rm mat}^2\rangle_{\rm rel} = \frac{1}{2\gamma_{cn}^2(1 - r_{cn}\gamma_{cn})}\frac{\mu_{cn}}{M+m}. \tag{5}$$

With the values from Eq. (2), we find $\langle r_{\rm mat}^2\rangle_{\rm rel} = 24(2)$ fm^2 where the error is from higher order corrections which are estimated to be of order 3%. Here, the matter radius of the core should be comparable to R and will therefore give a sizeable but smaller contribution to the total radius.

Three-body results.—The large two-body scattering length implies that the three-body sector (cnn) will display universal features associated with Efimov physics. From the Lagrangian (3), we can derive a set of two coupled integral equations for the cnn system. Here, the three-body coupling h contributes as well. (See Ref. [30] for more details.) The bound state solutions of these equations exhibit discrete scale invariance and the Efimov effect. At leading order, the spectrum is determined by the value of the scattering lengths in the two-body sector and one observable in the three-body sector which is used to fix the three-body coupling h [28].

For ^{62}Ca, the discrete scaling factor governing the energy spectrum is approximately 256. The exact scaling symmetry applies for deep states and in the unitary limit of infinite scattering length. For two levels near threshold, however, the ratio of their energies can be significantly smaller if one of the states is very close to the threshold (see the discussion in [5] for the case of identical bosons). In our case, the whole energy region between $S_n \approx$ 5–8 keV and the breakdown scale $S_{\rm deep} \approx 500$ keV is available for Efimov states in ^{62}Ca. It is thus conceivable

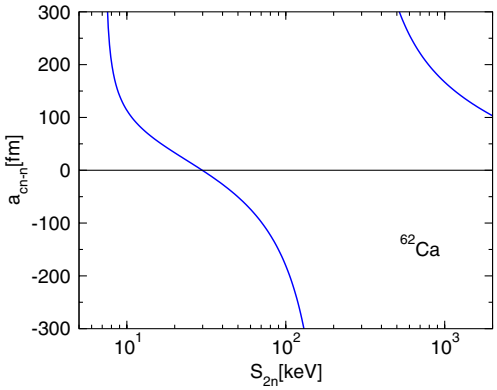

FIG. 2 (color online). The n-^{61}Ca scattering length as a function of the two-neutron separation energy S_{2n}.

that ^{62}Ca would display an excited Efimov state and unlikely that it would not display any Efimov states.

Another implication of the large scattering length in the cn system is that different low-energy three-body observables are correlated. This means that the measurement of one observable will uniquely determine all others up to corrections of order of R/a. In Fig. 2, we display the correlation between the two-neutron separation energy S_{2n} of ^{62}Ca and the n-^{61}Ca scattering length a_{cn-n}. The scattering length can take any value between $-\infty$ and ∞. When the binding energy of the halo state ^{62}Ca relative to the n-^{61}Ca threshold vanishes, the scattering length becomes infinite. The divergence in the n-^{61}Ca scattering around 230 keV indicates therefore the appearance of an additional state in the ^{62}Ca spectrum.

Four different matter radii can be calculated in the two-neutron halo system. The mean square (MS) radius between the two neutrons ($\langle r_{nn}^2 \rangle$), the MS radius between the core and one of the neutrons ($\langle r_{nc}^2 \rangle$), and radii that give the MS distance between the center-of-mass of the halo system and either one of the neutrons ($\langle r_n^2 \rangle$) or the core ($\langle r_c^2 \rangle$). These are correlated with other three-body observables. We have calculated the various matter radii using the methods of Ref. [31] and show their correlation with the two-neutron separation energy S_{2n} in Fig. 3.

The same type of correlation exists also for electromagnetic low-energy observables. In Ref. [30], the universal correlation between charge radius relative to the core and the two-neutron separation energy was studied as a function of the core-to-nucleon mass ratio and the one- and two-neutron separation energies of the halo nucleus. In Fig. 4, we show this correlation for ^{62}Ca. The total charge radius is expected to be dominated by the ^{60}Ca charge radius since the photon couples, at leading order, only to the charged core and not to the neutrons.

Summary.—We have calculated the S-wave phase shifts of the ^{60}Ca-n system using overlap functions obtained in coupled cluster theory. We analyzed the phase shift data and combined the results with halo EFT to predict universal features of the ^{61}Ca and ^{62}Ca systems. Our analysis indicates, despite uncertainties in the coupled cluster results due to truncation errors, a large scattering length in the ^{60}Ca-n system. Specifically, the S-wave scattering length is about 6 times larger than the effective range. We calculated the ^{61}Ca-n scattering length, and the matter and charge radii of ^{62}Ca. We have not considered the case of a negative scattering length. In this case, the ^{62}Ca system could be Borromean with none of the two-body subsystems being bound. The features of the ^{62}Ca observables would qualitatively remain the same as those depend mostly on the three-body parameter. From considerations based on the scaling factor of this system and the breakdown scale of halo EFT, we conclude that two Efimov states are possible in the ^{62}Ca system and that it is unlikely that this system possesses no bound state, i.e., is unbound.

Our results imply that ^{62}Ca is possibly the largest and heaviest halo nucleus in the chart of nuclei. We have shown that as a result a large number of observables would display characteristic features that could be used to test our

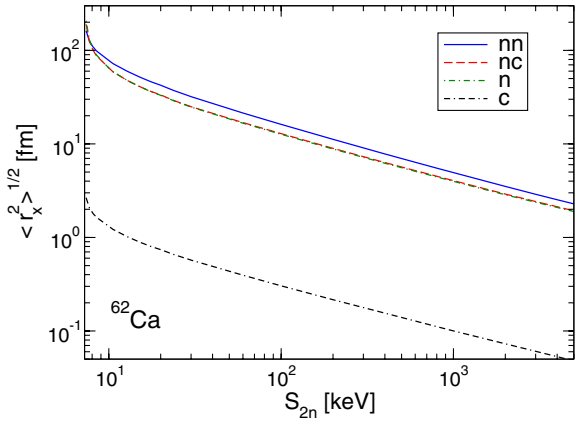

FIG. 3 (color online). Matter radii $\langle r_x^2 \rangle^{1/2}$ of the ^{62}Ca system for $x = nn$, nc, n, and c as a function of the two-neutron separation energy S_{2n}.

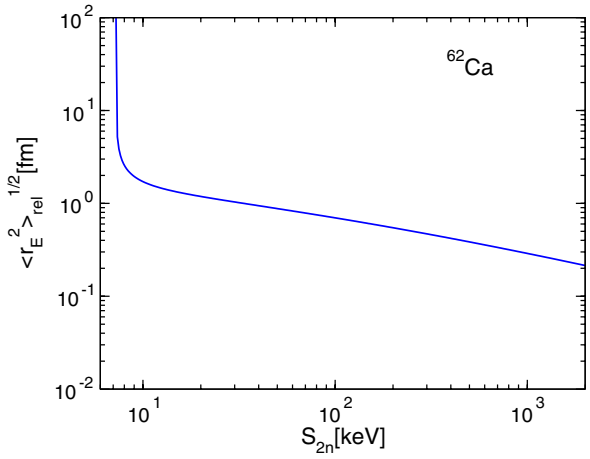

FIG. 4 (color online). The relative charge radius $\langle r_E^2 \rangle_{\rm rel}^{1/2}$ of the ^{62}Ca system as a function of the two-neutron separation energy S_{2n}.

hypothesis. Measurements of these observables will clearly pose a significant challenge for experiment. For example, ^{58}Ca is the heaviest calcium isotope that has been observed experimentally [32]. However, the planned facility for rare isotope beams might provide access to calcium isotopes as heavy as ^{68}Ca and thereby facilitate a test of our results [33].

We thank T. Papenbrock for useful discussions. This work was supported by the Office of Nuclear Physics, U.S. Department of Energy under Contracts No. DE-AC02-06CH11357, No. DE-AC05-00OR22725, and No. DE-SC0008499 (NUCLEI SciDAC), by the DFG and the NSFC through funds provided to the Sino-German CRC 110 "Symmetries and the emergence of structure in QCD,"and by the BMBF under Contract No. 05P12PDFTE. Computer time was provided by the Innovative and Novel Computational Impact of Theory and Experiment (INCITE) program. This research used computational resources of the Oak Ridge Leadership Computing Facility and of the National Center for Computational Sciences, the National Institute for Computational Science.

[1] M. V. Zhukov, B. V. Danilin, D. V. Fedorov, J. M. Bang, I. J. Thompson, and J. S. Vaagen, Phys. Rep. **231**, 151 (1993).
[2] A. S. Jensen, K. Riisager, D. V. Fedorov, and E. Garrido, Rev. Mod. Phys. **76**, 215 (2004).
[3] T. Frederico, A. Delfino, L. Tomio, and M. T. Yamashita, Prog. Part. Nucl. Phys. **67**, 939 (2012).
[4] K. Riisager, Phys. Scr. **T152**, 014001 (2013).
[5] E. Braaten and H.-W. Hammer, Phys. Rep. **428**, 259 (2006).
[6] L. Platter, Few-Body Syst. **46**, 139 (2009).
[7] V. Efimov, Phys. Lett. **33B**, 563 (1970).
[8] K. Tanaka *et al.*, Phys. Rev. Lett. **104**, 062701 (2010).
[9] W. Horiuchi and Y. Suzuki, Phys. Rev. C **74**, 034311 (2006).
[10] B. Acharya, C. Ji, and D. R. Phillips, Phys. Lett. B **723**, 196 (2013).
[11] A. Lapierre *et al.*, Phys. Rev. C **85**, 024317 (2012); A. T. Gallant *et al.*, Phys. Rev. Lett. **109**, 032506 (2012).
[12] J. D. Holt and A. Schwenk, J. Phys. G **39**, 085111 (2012).
[13] G. Hagen, M. Hjorth-Jensen, G. R. Jansen, R. Machleidt, and T. Papenbrock, Phys. Rev. Lett. **109**, 032502 (2012).
[14] W. Nazarewicz, J. Dobaczewski, T. Werner, J. Maruhn, P.-G. Reinhard, K. Rutz, C. Chinn, A. Umar, and M. Strayer, Phys. Rev. C **53**, 740 (1996); J. Erler, N. Birge, M. Kortelainen, W. Nazarewicz, E. Olsen, A. M. Perhac, and M. Stoitsov, Nature (London) **486**, 509 (2012).
[15] G. Hagen and N. Michel, Phys. Rev. C **86**, 021602(R) (2012).
[16] P. Navrátil and S. Quaglioni, Phys. Rev. Lett. **108**, 042503 (2012); S. Quaglioni and P. Navrátil, Phys. Rev. Lett. **101**, 092501 (2008).
[17] K. M. Nollett and R. B. Wiringa, Phys. Rev. C **83**, 041001 (2011); K. M. Nollett, S. C. Pieper, R. B. Wiringa, J. Carlson, and G. M. Hale, Phys. Rev. Lett. **99**, 022502 (2007).
[18] H. Dussan, S. J. Waldecker, W. H. Dickhoff, H. Muther, and A. Polls, Phys. Rev. C **84**, 044319 (2011); C. Barbieri and B. K. Jennings, Phys. Rev. C **72**, 014613 (2005).
[19] F. Coester, Nucl. Phys. **7**, 421 (1958); F. Coester and H. Kümmel, Nucl. Phys. **17**, 477 (1960); J. Čížek, J. Chem. Phys. **45**, 4256 (1966); Adv. Chem. Phys. **14**, 35 (1969); H. Kümmel, K. H. Lührmann, and J. G. Zabolitzky, Phys. Rep. **36**, 1 (1978).
[20] C. A. Bertulani, H.-W. Hammer, and U. Van Kolck, Nucl. Phys. **A712**, 37 (2002).
[21] P. F. Bedaque, H.-W. Hammer, and U. van Kolck, Phys. Lett. B **569**, 159 (2003).
[22] R. Machleidt and D. R. Entem, Phys. Rep. **503**, 1 (2011).
[23] D. R. Entem and R. Machleidt, Phys. Rev. C **68**, 041001 (R) (2003).
[24] J. W. Holt, N. Kaiser, and W. Weise, Phys. Rev. C **79**, 054331 (2009); **81**, 024002 (2010).
[25] D. Steppenbeck (private communication).
[26] R. J. Bartlett and M. Musiał, Rev. Mod. Phys. **79**, 291 (2007).
[27] Ø. Jensen, G. Hagen, T. Papenbrock, D. J. Dean, and J. S. Vaagen, Phys. Rev. C **82**, 014310 (2010).
[28] P. F. Bedaque, H.-W. Hammer, and U. van Kolck, Phys. Rev. Lett. **82**, 463 (1999).
[29] H.-W. Hammer and D. R. Phillips, Nucl. Phys. **A865**, 17 (2011).
[30] P. Hagen, H.-W. Hammer, and L. Platter, arXiv:1304.6516 [Eur. Phys. J. A (in preparation)].
[31] D. L. Canham and H.-W. Hammer, Eur. Phys. J. A **37**, 367 (2008).
[32] O. B. Tarasov *et al.*, Phys. Rev. Lett. **102**, 142501 (2009); O. B. Tarasov (private communication).
[33] B. Sherrill, *Proceedings of the Conference on Nuclear Structure 2012, Argonne National Laboratory, USA*.